



## HUMAN & MOUSE CELL LINES

Engineered to study multiple immune signaling pathways.

Transcription Factor, PRR, Cytokine, Autophagy and COVID-19 Reporter Cells  
ADCC, ADCC and Immune Checkpoint Cellular Assays



# The Journal of Immunology

RESEARCH ARTICLE | OCTOBER 15 2001

## AMD3100, a Potent and Specific Antagonist of the Stromal Cell-Derived Factor-1 Chemokine Receptor CXCR4, Inhibits Autoimmune Joint Inflammation in IFN- $\gamma$ Receptor-Deficient Mice<sup>1</sup> ✓

Patrick Matthys; ... et. al

*J Immunol* (2001) 167 (8): 4686–4692.

<https://doi.org/10.4049/jimmunol.167.8.4686>

### Related Content

Dual Effect of AMD3100, a CXCR4 Antagonist, on Bleomycin-Induced Lung Inflammation

*J Immunol* (May,2007)

CXCR4 antagonist AMD3100 mobilizes leukocytes from bone marrow and thymus to blood in mice (HEM2P.265)

*J Immunol* (May,2014)

A CXCR4-Dependent Chemorepellent Signal Contributes to the Emigration of Mature Single-Positive CD4 Cells from the Fetal Thymus

*J Immunol* (October,2005)

# AMD3100, a Potent and Specific Antagonist of the Stromal Cell-Derived Factor-1 Chemokine Receptor CXCR4, Inhibits Autoimmune Joint Inflammation in IFN- $\gamma$ Receptor-Deficient Mice<sup>1</sup>

Patrick Matthys,<sup>2,\*</sup> Sigrid Hatse,<sup>†</sup> Kurt Vermeire,<sup>\*</sup> Anja Wuyts,<sup>‡</sup> Gary Bridger,<sup>§</sup> Geoffrey W. Henson,<sup>§</sup> Erik De Clercq,<sup>†</sup> Alfons Billiau,<sup>\*</sup> and Dominique Schols<sup>†</sup>

Autoimmune collagen-induced arthritis (CIA) in IFN- $\gamma$ R-deficient DBA/1 mice was shown to be reduced in severity by treatment with the bicyclam derivative AMD3100, a specific antagonist of the interaction between the chemokine stromal cell-derived factor-1 (SDF-1) and its receptor CXCR4. The beneficial effect of the CXCR4 antagonist was demonstrable when treatment was initiated between the time of immunization and appearance of the first symptoms. Treatment also reduced the delayed-type hypersensitivity response to the autoantigen, collagen type II. These observations are indicative of an action on a late event in the pathogenesis, such as chemokine-mediated attraction of leukocytes toward joint tissues. The notion of SDF-1 involvement was further supported by the observation that exogenous SDF-1 injected in periarticular tissue elicited an inflammatory response that could be inhibited by AMD3100. The majority of leukocytes harvested from inflamed joints of mice with CIA were found to be Mac-1<sup>+</sup> and CXCR4<sup>+</sup>, and AMD3100 was demonstrated to interfere specifically with chemotaxis and Ca<sup>2+</sup> mobilization induced in vitro by SDF-1 on Mac-1<sup>+</sup>/CXCR4<sup>+</sup> splenocytes. We conclude that SDF-1 plays a central role in the pathogenesis of murine CIA, by attracting Mac-1<sup>+</sup>/CXCR4<sup>+</sup> cells to the inflamed joints. *The Journal of Immunology*, 2001, 167: 4686–4692.

Collagen II-induced arthritis (CIA)<sup>3</sup> in DBA/1 mice is an autoimmunity-driven inflammatory disease of joints, used as a study model for the pathogenesis of rheumatoid arthritis in man. A key event in this pathogenesis is the infiltration of the joint space and tissue with lymphocytes and mononuclear and polymorphonuclear phagocytes. Chemokines, produced by synoviocytes and inflammatory cells already present in the joints, are believed to play a central role in attracting additional leukocytes. One of these chemokines is stromal cell-derived factor-1 (SDF-1; recently renamed as CXCL12) (1). SDF-1 is rather unique among chemokines, in that it recognizes only a single receptor (CXCR4), which itself is only recognized by SDF-1 (2–4). The presence of both SDF-1 and CXCR4 in joints of rheumatoid arthritis patients is indirect evidence that they play an important role in the pathogenesis of arthritis (5, 6). In the present study, we have used a specific inhibitor of CXCR4 (AMD3100) to directly demonstrate the importance of SDF-1/CXCR4 interaction in CIA in mice. AMD3100 is a bicyclam derivative (Fig. 1) first described for its

potent activity against HIV infection (7, 8) and presently under investigation for clinical applicability in AIDS patients (9). It selectively antagonizes the CXCR4 (10, 11), which acts as a coreceptor for HIV (12). AMD3100 also inhibits the in vitro chemotactic and intracellular Ca<sup>2+</sup> flux responses of human monocytes to SDF-1 (10). This makes AMD3100 an ideal tool to evaluate the physiological and pathological importance of SDF-1/CXCR4 interactions. However, AMD3100 is rapidly cleared from the circulation, and treatment schedules in mice require the use of osmotic minipumps (13). This restricts the time of treatment to a maximum of 2 wk. Because development of CIA in wild-type DBA/1 mice takes on average 6 wk (14), we used IFN- $\gamma$ R-deficient (IFN- $\gamma$ R knockout (KO)) mice, as these are known to develop joint lesions that are pathologically identical with those in wild-type mice in much less time (average 3 wk) (14–16).

## Materials and Methods

### Induction of CIA

Chicken collagen type II (CII; EPC, Owensville, MO) was dissolved in 0.05 M acetic acid at 2 mg/ml and emulsified in an equal volume of CFA supplemented with 1.5 mg/ml heat-killed *Mycobacterium butyricum* (Difco, Detroit, MI). Eight- to 12-wk-old IFN- $\gamma$ R KO mice of DBA/1 strain (17) were sensitized with a single 100- $\mu$ l intradermal injection of the emulsion at the base of the tail. Mice were examined daily for signs of arthritis. The disease severity was recorded for each limb, as follows: score 0, normal; 1, redness and/or swelling in one joint; 2, redness and/or swelling in more than one joint; 3, redness and/or swelling in the entire paw; 4, deformity and/or ankylosis. In each experiment, mice were age and sex matched in the different groups.

### Histology

Fore- and hind limbs (ankles and interphalanges) were fixed in 10% Formalin and decalcified with formic acid. Paraffin sections (4  $\mu$ m) were stained with H&E. Severity of arthritis was evaluated blindly, using three parameters: infiltration of mono- and polymorphonuclear cells, hyperplasia of the synovium, and pannus formation. Each parameter was scored on a

Laboratories of \*Immunobiology, <sup>†</sup>Experimental Chemotherapy, and <sup>‡</sup>Molecular Immunology, Rega Institute for Medical Research, Katholieke Universiteit Leuven, Leuven, Belgium; and <sup>§</sup>AnorMed, Langley, British Columbia, Canada

Received for publication May 11, 2001. Accepted for publication August 2, 2001.

The costs of publication of this article were defrayed in part by the payment of page charges. This article must therefore be hereby marked *advertisement* in accordance with 18 U.S.C. Section 1734 solely to indicate this fact.

<sup>1</sup> This work was supported by grants from the Fund for Scientific Research Flanders (FWO, Vlaanderen), from the Regional Government of Flanders (GOA Program), and from the Belgian Federal Government (Interuniversity Network for Fundamental Research, IUAP). P.M., S.H., and A.W. are postdoctoral research fellows of the FWO.

<sup>2</sup> Address correspondence and reprint requests to Dr. Patrick Matthys, Rega Institute, University of Leuven, Minderbroedersstraat 10, B-3000 Leuven, Belgium. E-mail address: Patrick.Matthys@rega.kuleuven.ac.be

<sup>3</sup> Abbreviations used in this paper: CIA, collagen-induced arthritis;  $\beta_2$ m,  $\beta_2$ -microglobulin; CII, collagen type II; DTH, delayed-type hypersensitivity; KO, knockout; SDF-1, stromal cell-derived factor-1.

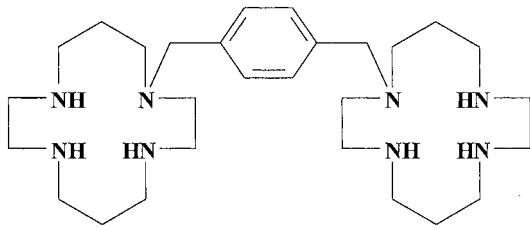


**FIGURE 1.** Structure of AMD3100, 1,1'-[1,4-phenylenebis(methylene)]-bis-1,4,8,11-tetraazacyclotetradecane.

scale from 0 to 3: score 0 (absent), score 1 (weak), score 2 (moderate), score 3 (severe).

#### Treatments with AMD3100

AMD3100 treatment schedules were virtually identical with those developed on the basis of careful pharmacokinetic evaluation by Datema et al. (13). We used the same Alzet osmotic minipumps (Alza, Palo Alto, CA), implanted dorsolaterally under the skin. All mice were anesthetized with 200  $\mu$ l of a solution in PBS of 0.2% Rompun (Bayer, Brussels, Belgium) and 1% Ketalar (Parke-Davis, Zaventem, Belgium). In most experiments, number 2002 pumps (delivering 0.5  $\mu$ l/h for 14 days) were used and were filled with either 3 or 10 mg of AMD3100 in 200  $\mu$ l of PBS (AMD3100 pump, delivering the drug at a rate of, respectively, 180 or 600  $\mu$ g/day). According to Datema et al. (13), this corresponds to steady serum levels of, respectively, 0.3 or 1  $\mu$ g/ml. In experiment 2 of Fig. 4B, number 1007D pumps were used and delivered AMD3100 at a rate of 576  $\mu$ g/day for 7 days. In two experiments (Fig. 2, A and D), groups of mice implanted with pumps containing PBS only (without AMD3100) were included. All other untreated mice were anesthetized like treated ones, but were not implanted with pumps.

#### Serum anti-CII Ab levels and delayed-type hypersensitivity (DTH)

Individual sera were tested for the amount of Abs directed to chicken CII by ELISA, as described (14). For evaluation of DTH reactivity, mice were challenged in the right footpad with 10  $\mu$ g of chicken CII in 20  $\mu$ l of PBS. The left footpad received 20  $\mu$ l of PBS. DTH response was measured as percentage of swelling at 24 and 48 h postchallenge.

#### Flow cytometric analysis

Spleens were diced and passed through cell strainers (BD Labware, Franklin Lakes, NJ). Blood, taken by heart puncture, was collected on heparin. Cells from joint cavities were obtained from an opening that was made with a 25-gauge needle in the skin on the dorsal side of the foot, just distally from the interphalangeal space. Eighty microliters of cold PBS was injected in the interphalangeal spaces, the needle being inserted on the dorsal side of the foot and oriented from proximal to distal. Fluid exiting spontaneously from the distal opening was collected and was only used when it was found to contain <10% of RBCs. Erythrocytes were removed from blood and splenocyte suspensions by lysis with  $\text{NH}_4\text{Cl}$  (0.83% in 0.01 M Tris-HCl, pH 7.2; two consecutive incubations of 5 and 3 min, 37°C). Remaining cells were washed, resuspended in cold PBS, and counted. Aliquots of  $2 \times 10^5$  cells in 0.2 ml were preincubated (30 min) with a FcR-blocking Ab (2.4G2, 1  $\mu$ g/ml; BD Pharmingen, San Diego, CA) and then stained for 30 min with FITC-conjugated anti-Mac-1 (CD11b) Ab and PE-conjugated anti-CXCR4 (12G5; R&D Systems Europe, Abingdon, U.K.). Simultest control  $\gamma_1/\gamma_{2a}$  (BD Biosciences, San Jose, CA) was used as isotype control. Cells were analyzed by a FACScan flow cytometer (BD Biosciences).

#### Measurement of intracellular calcium flux

An enriched Mac-1<sup>+</sup> cell population was obtained by depletion of T and B cells from splenocytes using CD90 (Thy-1.2) and CD45R (B220) microbeads (Miltenyi Biotec, Bergisch Gladbach, Germany); the purity was analyzed by flow cytometry. Mac-1<sup>+</sup> cells were loaded with the fluorescent calcium indicator Fluo-3 acetoxyethyl (Molecular Probes, Leiden, The Netherlands) at 4  $\mu$ M for 45 min at room temperature. After thorough washing with HBSS containing 20 mM HEPES and 0.2% BSA (pH 7.4), the cells were resuspended in the same buffer and were seeded at  $3 \times 10^5$  cells/well into a 96-well plate, containing AMD3100 at different concentrations. After preincubation of the cells for 20 min in the presence of

AMD3100, 50 ng/ml murine SDF-1 (R&D Systems) was added, and the fluorescence in function of time was monitored simultaneously in all wells by a Fluorometric Imaging Plate Reader (Molecular Devices, Sunnyvale, CA).

#### Chemotactic assay

SDF-1-induced cell migration was assessed using 5- $\mu$ m-pore Transwell filter membranes (Costar, Boston, MA). The membrane inserts were placed in the wells of a 24-well plate, containing 600  $\mu$ l of HBSS (see above) with murine SDF-1. After preincubation with AMD3100 at different concentrations,  $1 \times 10^6$  purified Mac-1<sup>+</sup> cells in 100  $\mu$ l of buffer were loaded into each Transwell filter. The plate was then incubated at 37°C for 3.5 h, whereafter the filter inserts were carefully removed and the migrated cells were collected from the wells and counted in a flow cytometer. Chemotactic index is the number of migrated cells obtained with 0.1  $\mu$ g/ml SDF-1 divided by the number of migrated cells in the negative control (without SDF-1). Migrated cells were characterized after centrifugation by cyto-spin (Shandon, Cheshire, U.K.) and staining with Hemacolor (Merck, Darmstadt, Germany).

#### Semiquantitative analysis of SDF-1 mRNA by RT-PCR

The skin was removed from mouse hind limbs, and ankle joints were dissected. Joint tissues were snap frozen in liquid nitrogen and pulverized. RNA was extracted by the TRIzol Reagent method (Life Technologies, Gaithersburg, MD). First-strand cDNA was synthesized using 1  $\mu$ g of total RNA and 4.5 U of RAV-2 reverse transcriptase (Amersham, Aylesbury, U.K.). The reaction mixture was incubated for 80 min at 42°C, followed by a denaturation step of 5 min at 95°C. As an external control for the amount of RNA in the different samples,  $\beta_2$ -microglobulin ( $\beta_2$ m) mRNA was first quantitated by PCR with the primers  $\beta_2$ mFOR (5'-CTGACCGGCTG TATGCTATCC-3') and  $\beta_2$ mBACK (5'-CATGTCTCGATCCCAGTA GACGG-3') using 0.25 U SuperTaq DNA polymerase (HT Biotechnology, Cambridge, U.K.). After determining the volumes of first-strand cDNA sample that gave the same yield of  $\beta_2$ m PCR product, SDF-1 mRNA was quantified with SDF-1-specific primers SDF-1FOR (5'-TCAGCCTGAGC TACCGATGC-3') and SDF-1BACK (5'-ACGGATGTCACGCTTC CTCG-3'). All PCR were performed in 50- $\mu$ l reaction mixtures on a GeneAmp PCR System 2400 (PerkinElmer, Norwalk, CT) for 30 cycles ( $\beta_2$ m and SDF-1), in which each cycle consists of 30 s at 95°C, 30 s at 64°C, and 30 s at 72°C, with a final extension step of 5 min at 72°C. Equal amounts of PCR products (for  $\beta_2$ m and SDF-1) of the samples were analyzed on 1.5% agarose gels and stained with ethidium bromide.

#### In vivo effects of SDF-1

Murine SDF-1 (1  $\mu$ g in 20  $\mu$ l of PBS) was injected in the right footpads of immunized mice. Redness and swelling reaction were recorded at different time points. The swelling reaction was measured by calipers and expressed as the mean percentage of increase in footpad thickness relative to the thickness before the SDF-1 challenge. At 24 or 48 h postchallenge, cells from the inflamed area were obtained in a similar way as described for arthritic joints, and were stained with Hemacolor after centrifugation by cyto-spin.

#### Statistical analyses

The Mann-Whitney *U* test, Student's *t* test, and the log rank test for survival curves (referred to in Ref. 14) were used as indicated.

## Results

In a first experiment, IFN- $\gamma$ R KO mice were implanted with osmotic minipumps releasing AMD3100 at a rate of 180  $\mu$ g/day for 14 days (see *Materials and Methods*). The treatment regime was adapted from experiments in which AMD3100 successfully inhibited HIV infection in SCID-hu Thy/Liv mice (13). Two additional groups of control mice, either implanted with pumps containing PBS or not implanted, were included. One day after pump implantation, all mice were immunized with CII in CFA, and examined daily for clinical signs of arthritis. In control mice and in mice receiving PBS, the symptoms of arthritis started to appear as early as day 19 (Fig. 2A). In AMD3100-treated mice, the first symptoms appeared about 2 wk later. By that time, nearly 50% of the control and PBS-treated mice had developed arthritis. The mean day of disease onset in AMD3100-treated mice was significantly different

from that in control or PBS-treated mice ( $p < 0.05$ , Mann-Whitney  $U$  test); mean arthritis scores of AMD3100 and PBS-treated mice were significantly different ( $p < 0.05$ ) in the time interval from day 28 to day 37. The differences in disease onset times and scores of arthritis were confirmed in an additional experiment (Fig. 2B). The clinical scores of arthritis were substantially lower in AMD3100-treated mice (Fig. 2B,  $p < 0.03$  from day 19 to day 40, Mann-Whitney  $U$  test).

The effect of treatment with AMD3100, initiated at a later time point, was also investigated. In two independent experiments, mice were implanted with AMD3100 pumps on day 7 postimmunization. Here again, the incidence of arthritis was lower, the onset was delayed, and the clinical disease scores were significantly lower in mice treated with AMD3100 (Fig. 2, C and D). These experiments were terminated on days 25 and 20 to allow for, respectively, histological examination and testing DTH (see below). The joints

were analyzed histologically at this rather early time point, to ascertain that the protective effect of AMD3100 on the clinical symptoms of arthritis correlated with inhibition of tissue damage. The data, summarized in the inset of Fig. 2C, confirmed the protective effect of AMD3100 against the development of arthritis: infiltration of mono- and polymorphonuclear cells, hyperplasia of the synovium, and pannus formation were all dramatically reduced in treated mice.

Finally, we assessed whether AMD3100 could control CIA when administered at the time of disease onset. To this end, CII-immunized mice were divided into two groups at the time when clinical symptoms of arthritis started to appear. In one group, the mice were implanted with minipumps containing AMD3100, whereas in the other group the mice were left untreated. In a first experiment, in which mice were treated with the regular dose of AMD3100 (180  $\mu\text{g}/\text{day}$  for 14 days), the average clinical score did

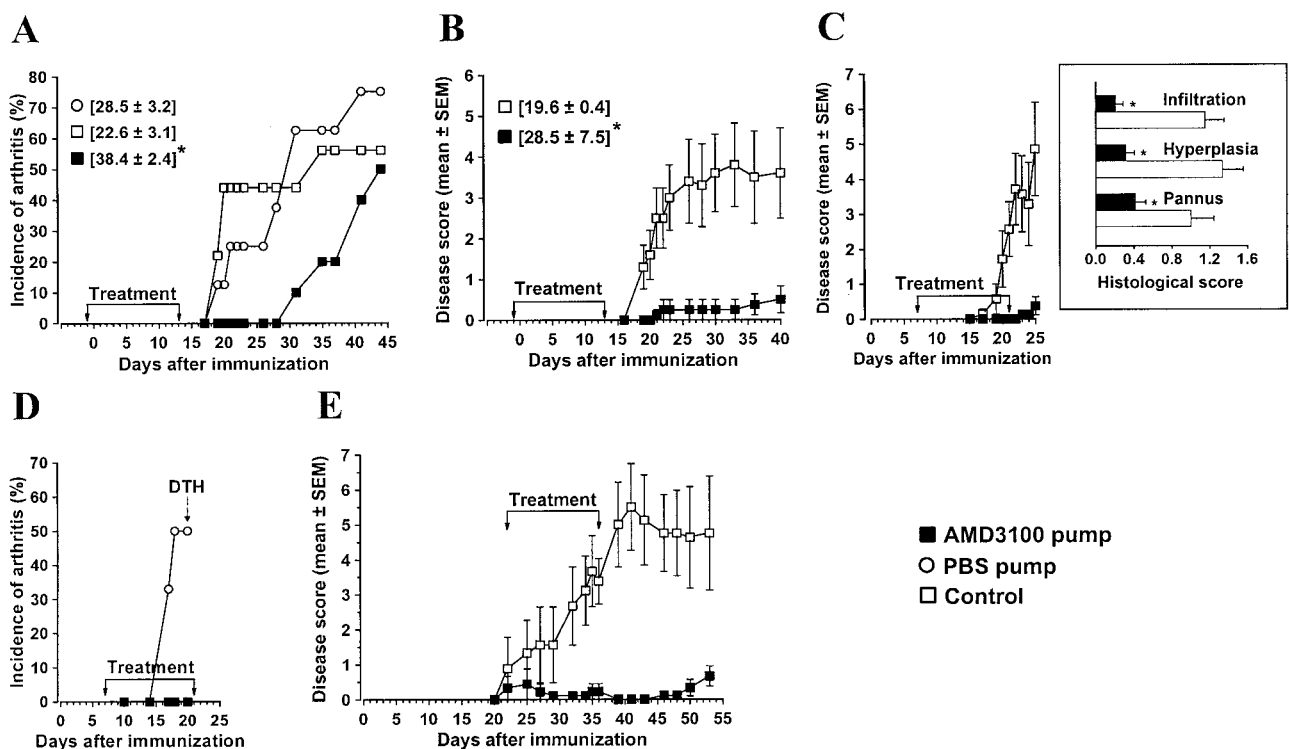


**FIGURE 2.** Inhibition of CIA by treatment with AMD3100 (data of five independent experiments). Mice were immunized with CII in CFA on day 0 and implanted on day  $-1$  (A and B), day 7 (C and D), or day 22 (E) with osmotic minipumps delivering AMD3100 at a rate of 180  $\mu\text{g}/\text{day}$  (A–D) or 600  $\mu\text{g}/\text{day}$  (E) during a period of 14 days, as indicated (treatment). As controls, groups of mice were implanted with minipumps containing an equal volume of PBS, or were left untreated. Either the incidence of arthritis (A and D) or disease scores (B, C, and E) are shown. A, On day  $-1$ , two groups of mice received minipumps containing either AMD3100 ( $n = 10$ ) or PBS ( $n = 8$ ). Control mice ( $n = 9$ ) received no pumps. The graph shows cumulative incidence of arthritis in each group. In brackets: mean days of onset of arthritis (numbers of affected mice were 5, 6, and 5 for, respectively, AMD3100, PBS, and control; \*,  $p < 0.05$  for comparison by Mann-Whitney  $U$  test with PBS or control). B, Same treatment procedure as in A. Each point represents the mean score  $\pm$  SEM for eight AMD3100-treated and 10 control mice. The differences in disease scores reached statistical significance from day 19 until the end of the experiment ( $p < 0.03$ , Mann-Whitney  $U$  test). In brackets: mean days of onset of arthritis (\*,  $p < 0.05$  for comparison by Mann-Whitney  $U$  test with control). Statistical significance for the difference in cumulative incidence between AMD3100-treated and control or PBS group was tested with the log rank test and revealed  $\chi^2$  values of 2.8 and 4.4 for the two independent experiments, A and B, respectively, yielding an overall  $p$  value  $< 0.05$ . C, Two groups of mice were either left untreated (control,  $n = 7$ ) or implanted with AMD3100-containing pumps ( $n = 8$ ) on day 7. The graph shows mean disease scores  $\pm$  SEM (significantly different from day 21 onward;  $p < 0.02$ , Mann-Whitney  $U$  test). Inset, Six mice of each group (including the only two mice with clinical symptoms in the AMD3100 group) were sacrificed on day 25. The forepaws, toes, and ankle sections were scored histologically for three parameters of arthritis. Bars represent averages  $\pm$  SEM of at least 27 sections of six mice. \*,  $p < 0.05$  (infiltration),  $p < 0.0001$  (hyperplasia),  $p < 0.02$  (pannus); Student's  $t$  test. D, Two groups of six mice were treated with AMD3100- or PBS-containing pumps on day 7 postimmunization with CII. On day 20, clinical symptoms of arthritis were observed in three control mice, but not in animals treated with AMD3100. On that day, mice were subjected to DTH testing, as further explained in Fig. 4B, experiment 1. E, Eighteen mice were immunized with CII in CFA. Clinical symptoms of arthritis started to appear on day 22. Mice were then divided into two groups such that an equal incidence had been reached in both groups, and one group was implanted with AMD3100-containing minipumps delivering 600  $\mu\text{g}/\text{day}$  for 14 days. The graph shows mean disease scores  $\pm$  SEM (significantly different from day 32 until the end of the experiment, i.e.,  $p < 0.05$  (days 32 and 34),  $p < 0.001$  (days 35–46),  $p < 0.02$  (days 48–53); Mann-Whitney  $U$  test).



remain below that in the control group, although the difference was not statistically significant (mean end scores  $\pm$  SEM on day 40 postimmunization:  $0.6 \pm 0.3$  for 10 AMD3100-treated mice vs  $2.3 \pm 0.9$  for 10 control mice). In a second experiment, the dose of AMD3100 was increased to  $600 \mu\text{g}/\text{day}$  for 14 days (see *Materials and Methods*) and pumps were implanted at the time of disease onset, i.e., on day 22 postimmunization. As can be seen in Fig. 2E, the clinical scores in treated mice were significantly lower than in control mice. Whereas control mice showed scores gradually increasing to a maximum averaging 5.5, treated mice remained below score 1 throughout the experiment.

We also measured body weight changes to evaluate potential toxicity of the compound. In fact, AMD3100-treated mice gained more weight than the controls (data not shown), suggesting that reduced CIA scores were not due to possible toxic effects of the compound (18). Moreover, spleens, lymph nodes, livers, kidneys, lungs, hearts, and intestines of AMD3100-treated mice had normal histological appearance (data not shown). The protective effect of AMD3100 on the clinical severity of arthritis was confirmed by histological examination (day 53). Representative images are shown in Fig. 3. Treated mice showed a marked decrease in cellular infiltration and hyperplasia of the synovium. The mean joint scores of AMD3100-treated vs control mice ( $n = 16$  limbs from four mice) were, respectively,  $0.25 \pm 0.12$  vs  $2.06 \pm 0.17$  for infiltration ( $p < 0.00001$ , Student's  $t$  test) and  $0.63 \pm 0.18$  vs  $2.25 \pm 0.19$  for hyperplasia ( $p < 0.0001$ ). Moreover, a moderate to severe pannus formation, which is often seen at this stage of the disease (Fig. 3C), was barely detectable in AMD3100-treated mice (6% in limbs of treated mice vs 81% in those of control mice; mean scores were, respectively,  $0.50 \pm 0.16$  vs  $2.19 \pm 0.19$ ,  $p < 0.00001$ ).

To gain more insight in the mechanism underlying the protective effect of AMD3100 on the development of CIA, humoral and cellular immunity against CII were studied. The humoral response to CII was assessed by measuring anti-CII Abs (total IgG) in the sera obtained from the mice of the experiment described in Fig. 2A. Serum levels of anti-CII Abs (Fig. 4A) were not affected by AMD3100 treatment. The cellular immune response to CII was examined by measuring DTH reactivity against CII injected in the footpad. On day 7 postimmunization with CII in CFA, treatment with either AMD3100 or PBS was initiated. On day 20, no clinical signs of arthritis were detectable in the AMD3100-treated mice, whereas by that time 50% of the mice in the PBS group had developed limb inflammation. On this day, mice without clinical swelling of the hind limbs were selected from each group and challenged with CII by injection in the footpad. As shown in Fig. 4B (Expt. 1), in PBS pump-treated mice, a distinct DTH reaction was observed at 24 and 48 h postchallenge. The swelling reaction was significantly less pronounced in the mice that had received AMD3100. Importantly, a reduced swelling reaction was also seen in another experiment in which AMD3100 treatment was started as late as day 25 postimmunization, i.e., 2 days before the challenge with CII (Fig. 4, B (Expt. 2) and C).

As the anti-HIV effect of AMD3100 originates from specific binding to the chemokine receptor CXCR4 (10, 11) (vide infra), the inhibitory effect of AMD3100 on CIA and on the DTH reaction against CII may be due to interference with migration of CXCR4<sup>+</sup> leukocytes into the inflamed tissues. Therefore, we examined the expression of CXCR4 on splenocytes, on blood leukocytes, and on cells obtained from the arthritic joints of mice with CIA. As shown in Fig. 5, all three cell populations strongly expressed CXCR4. In accordance with the established involvement of Mac-1<sup>+</sup> (CD11b<sup>+</sup>) cells in the pathogenesis of CIA (16, 19), >90% of the cells harvested from arthritic joint cavities appeared to be Mac-1<sup>+</sup>.

Interestingly, a pattern of CXCR4 and Mac-1 expression similar to that in the arthritic joints was seen in inflamed footpads after a CII challenge to elicit DTH.

Because CXCR4-expressing Mac-1<sup>+</sup> cells were abundantly present in arthritic joints, the protective effect of AMD3100 in CIA could possibly be explained by inhibition of Mac-1<sup>+</sup> leukocyte migration through interference with the chemotactic activity of the natural CXCR4 ligand, SDF-1. To document this possibility, we tested the ability of AMD3100 to interfere with SDF-1-induced signaling in Mac-1<sup>+</sup> splenocytes in vitro. A highly enriched (>96%) Mac-1<sup>+</sup> cell population was preincubated with AMD3100 and subsequently stimulated with murine SDF-1. The

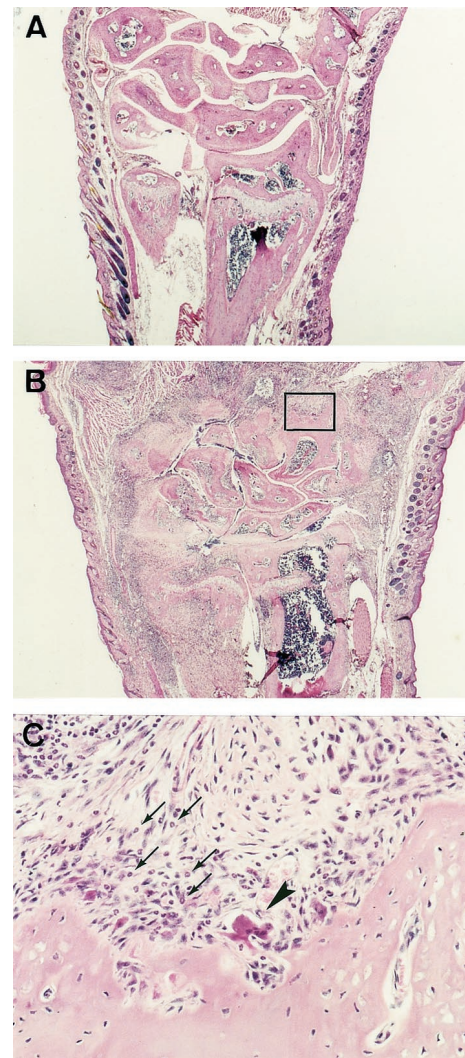


**FIGURE 3.** Joint histology of AMD3100-treated and untreated mice. Four mice in each group of the experiment shown in Fig. 2E were randomly selected on day 53, and sections of their fore- and hind limbs were examined. All 16 sections were blindly scored, and results are described in the text. Representative histological images of the metatarsalia are shown. A and B, Joints of an AMD3100-treated and untreated mouse. Synovia of untreated mice (B) are severely infiltrated by leukocytes (close-up in C). Joints of AMD3100-treated mice (A) have a normal histological appearance without infiltration of immunocompetent cells. Magnification,  $\times 21$ . C, Detail of the area indicated by the box in B, showing hyperplasia of the synovium and pannus formation penetrating into the bone tissue. Note the presence of mono- and polymorphonuclear cells (arrows) as well as a multinucleated or osteoclast-like cell (arrowhead). Moderate to severe pannus formation was seen in 81% of limb sections of untreated mice vs 6% of those of AMD3100-treated mice ( $n = 16$ ). Magnification,  $\times 136$ .

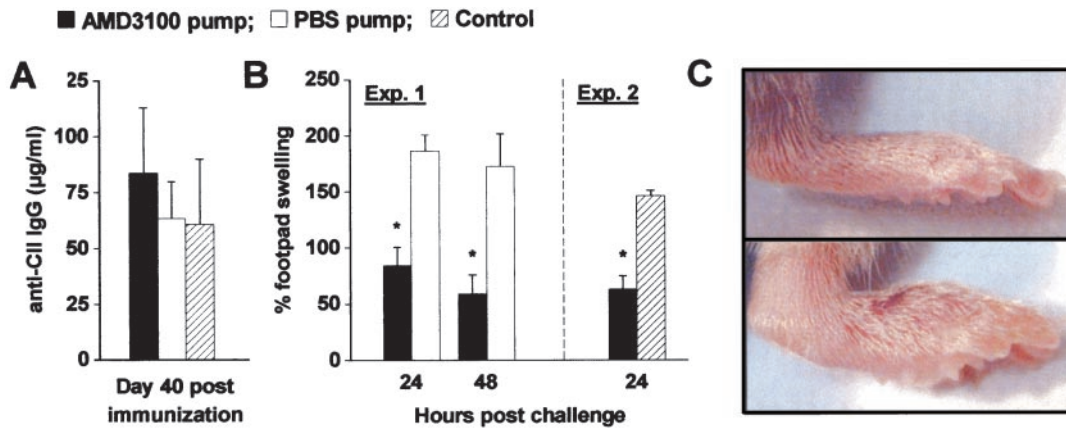


**FIGURE 4.** AMD3100 interferes with the cellular (DTH), but not with the humoral immune response to CII in CIA. **A**, Serum levels of anti-CII Abs (total IgG) on day 40 postimmunization. Mice were immunized and treated as described in Fig. 2A. Bars represent averages  $\pm$  SEM for 8–10 mice. Abs were undetectable on day 0. **B**, DTH reactivity to CII. Experiment 1, Two groups of six mice were immunized as described in Fig. 2D. On day 20, mice ( $n = 4$  for each group) were challenged by injection in the footpad of 10  $\mu$ g of CII (right footpad) or vehicle (left footpad). Experiment 2, Two groups of four mice were immunized with CII in CFA (day 0). On day 25, one group was implanted with AMD3100-containing pumps delivering 576  $\mu$ g/day for 7 days, while the other group was left untreated. On day 27, all mice were challenged for DTH by injection of 10  $\mu$ g of CII in the footpad. DTH responses were measured as the percentage of swelling at the indicated times. Bars represent averages  $\pm$  SEM; \*,  $p < 0.05$  for comparison with PBS pump (Mann-Whitney  $U$  test). **C**, Images of CII-elicited DTH reaction in AMD3100-treated (*top*) and nontreated (*bottom*) mice from Expt. 2 in **B**. Pictures of footpad-swelling reactions were taken 24 h postchallenge.

intracellular  $\text{Ca}^{2+}$  mobilization was dose dependently inhibited by AMD3100 (Fig. 6A). Then, we also investigated the capacity of AMD3100 to inhibit SDF-1-induced migration of  $\text{Mac-1}^{+}$  cells (Fig. 6B). Clearly, murine SDF-1 elicited a strong chemotactic response on  $\text{Mac-1}^{+}$  cells: at 0.1 and 0.5  $\mu$ g/ml, SDF-1 triggered migration of, respectively, 14 and 30% of the cells, with a chemotactic index of 30 (for 0.1  $\mu$ g/ml SDF-1). Moreover, the percentage of cells that migrated in response to SDF-1 gradually decreased when the cells were preincubated with AMD3100 at increasing concentrations (Fig. 6B). Further characterization of the cells that were attracted by SDF-1 revealed that  $>95\%$  stained positively for both Mac-1 and CXCR4. As shown in Fig. 6C, the vast majority of migrated cells contained a ring-shaped nucleus, a characteristic attributed to immature monocytes and neutrophils (20). It is important to note that cells of a similar phenotype are present in the synovia of arthritic joints (Fig. 3C).

Evidence for active production of SDF-1 in inflamed joints was obtained by measurement of SDF-1 mRNA in joint tissue extract (Fig. 7). Expression was present in joint tissues of mice free of symptoms (either naive or immunized mice), but was more pronounced in inflamed joints. We next tested in vivo interference of AMD3100 with SDF-1-induced cell migration in a footpad-swelling test. Preliminary tests had established that local injection of murine SDF-1 (doses of 1, 5, or 7.5  $\mu$ g) in the footpad induces redness and swelling in mice that had previously been immunized with CII in CFA. Therefore, on day 19 postimmunization, mice were given an i.p. injection of AMD3100 (25  $\mu$ g in 100  $\mu$ l of PBS), followed by injection of 1  $\mu$ g of SDF-1 in the right footpad; controls received PBS without the drug and were similarly challenged with SDF-1. Increases of footpad thickness (mean percentage  $\pm$  SEM) were most pronounced at 4 h after SDF-1 injection and were  $9.1 \pm 3.7$  in treated vs  $36.8 \pm 6.5$  in controls ( $n = 4$ ;  $p < 0.05$  by Mann-Whitney  $U$  test). Fluid aspirated from the footpad of controls contained leukocytes (mainly polymorphonuclear cells), whereas virtually no cells could be obtained from the footpads of AMD3100-treated mice.

## Discussion

AMD3100 is a specific CXCR4 antagonist: it does not interact with CCR1 to CCR8, CXCR1, CXCR2, Bob/gpr15, V28, APJ,

US28, NK1 tachykinin (substance P) receptor, fMLP receptor, and C5a receptor (Refs. 10 and 11, and unpublished data). Therefore, our data strongly suggest that the protective effect of AMD3100 in murine CIA is due to interference with the activity of SDF-1, endogenously produced during development of the disease. As evident from the inhibitory effect of AMD3100 on the intracellular  $\text{Ca}^{+}$  flux and chemotactic responses of  $\text{Mac-1}^{+}$  splenocytes to SDF-1, a cell population expressing this marker can be surmised to represent the in vivo target for SDF-1 and, hence, for the protective effect of AMD3100. Such cells, mainly consisting of immature and mature monocytes/macrophages and neutrophils, were previously identified to play a central role in CIA pathogenesis (16, 19). Conceivably, they constitute the precursors of tissue-infiltrating and destructive phagocytes, although it is not excluded that they also act as regulators of T or B lymphocytes. In fact, all cells in joint cavities of the arthritic mice were  $\text{Mac-1}^{+}$ . In addition, a substantial fraction of these  $\text{Mac-1}^{+}$  cells strongly expressed CXCR4. However, it cannot be excluded that other  $\text{CXCR4}^{+}$  cells, which do not express Mac-1, exist in the synovial membrane of arthritic

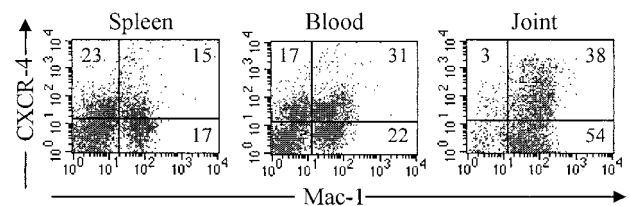


**FIGURE 5.** Highly CXCR4-positive cells are present in arthritic joints. Mice were immunized with CII in CFA on day 0. On day 27, splenocytes, blood cells, and cells from arthritic ankles were obtained. After preincubation with FcR-blocking Ab, cells were stained with FITC-conjugated anti-Mac-1 (CD11b) and PE-conjugated anti-CXCR4 and analyzed by flow cytometry. The percentages of cells in each quadrant are indicated. Data shown for spleen and blood cells are from a single mouse and are representative for data obtained in 10 animals. The data for the joint are from a pool of cells harvested from three arthritic ankles. A similar staining pattern was seen on day 45 in a separate experiment. Note the high proportion of  $\text{Mac-1}^{+}$  cells in the arthritic joints ( $>90\%$ ); a substantial fraction of these cells was strongly positive for expression of CXCR4. No cells could be isolated from clinically symptom-free joints.



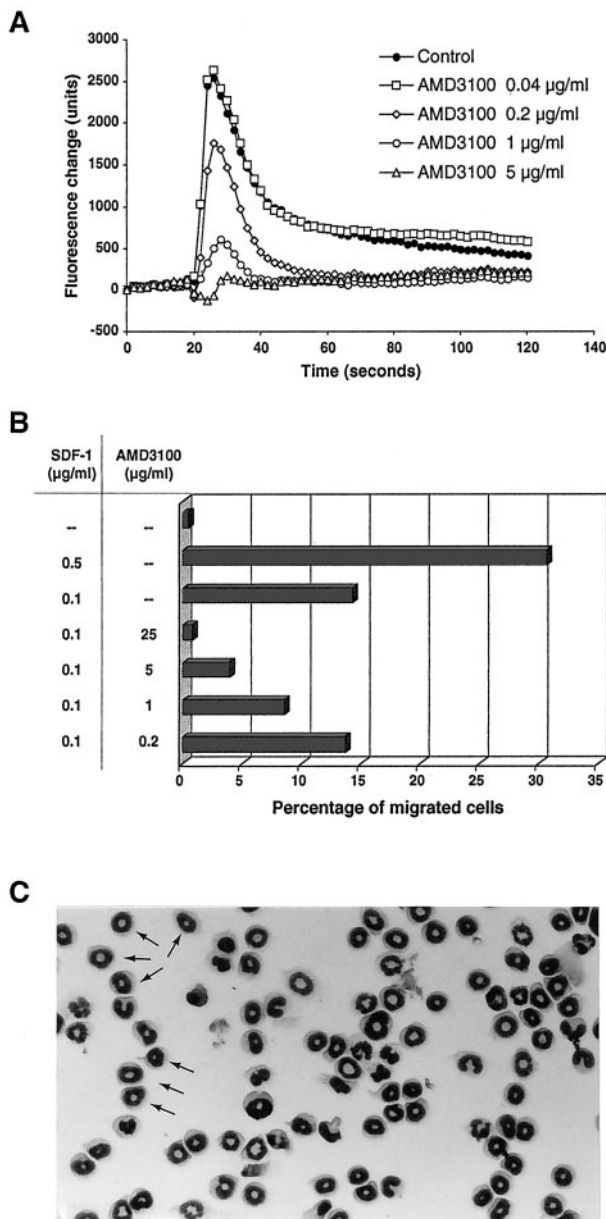


**FIGURE 6.** Inhibition by AMD3100 of SDF-1-elicited intracellular  $\text{Ca}^{2+}$  fluxes and chemotaxis on a Mac-1<sup>+</sup> cell-enriched (>96%) population. On day 18 postimmunization with CII in CFA, spleens of three mice were pooled, and Mac-1<sup>+</sup> (CD11b<sup>+</sup>) cells were isolated, as described in *Materials and Methods*. *A*, Calcium flux: Mac-1<sup>+</sup> cells were loaded with the fluorescent calcium indicator Fluo-3. After preincubation of the cells for 20 min with AMD3100 at the indicated concentrations, 50 ng/ml murine SDF-1 was added simultaneously in all wells, and the fluorescence was monitored in function of time. Each data point represents the average value of the fluorescence measured in quadruplicate microplate wells. One representative experiment of two is shown. *B*, Chemotaxis: Mac-1<sup>+</sup> cell samples were preincubated for 10 min with AMD3100 at the indicated concentrations. Then, 5- $\mu\text{m}$  filter inserts were loaded with  $1 \times 10^6$  cells and transferred to a 24-well plate containing 0, 0.1, or 0.5  $\mu\text{g}/\text{ml}$  murine SDF-1 in 600  $\mu\text{l}$  of buffer. Transmigration of the Mac-1<sup>+</sup> cells was followed microscopically and was found to initiate after 2 h. After 3.5 h of incubation, the membrane inserts were removed and the cells in the wells were collected and counted by flow cytometry. The data of one representative experiment of three are shown: the mean percentages of inhibition of cell migration by 25 and 5  $\mu\text{g}/\text{ml}$  AMD3100 were  $97.6 \pm 0.3$  and  $76.7 \pm 5.5$ , respectively. *C*, Cytospin preparation of cells having crossed the Transwell filter membrane following exposure to 0.5  $\mu\text{g}/\text{ml}$  SDF-1. Note the large proportion of cells with a ring-shaped nucleus (some of them are indicated by arrows). Hemacolor staining; magnification,  $\times 223$ .

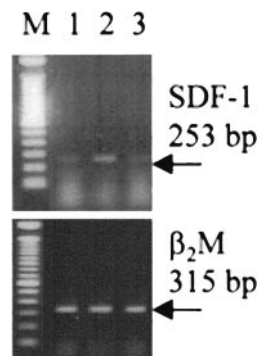


**FIGURE 7.** The presence of SDF-1 mRNA levels in joint extracts of mice. On day 21 postimmunization with CII in CFA, mice without (lane 1) or with clinical symptoms of arthritis (lane 2) were selected, and ankle joint extracts were obtained, as described in *Materials and Methods*. Joint tissues of naive mice were included (lane 3). In each group, joint extracts ( $n = 4$ ) of two to four mice were pooled, and mRNA levels were analyzed using RT-PCR and  $\beta_2\text{m}$  as housekeeping gene. M, The 100-bp marker.

joint. Buckley et al. (5) recently reported, in rheumatoid arthritis, CXCR4 expression by various synovial cells, including T and B cells, macrophages, and synoviocytes.

SDF-1 mRNA, unlike that of most other chemokines, is constitutively expressed in a wide range of tissues (2). Overexpression has recently been reported to occur in cultured synoviocytes of rheumatoid arthritis patients, but, interestingly, not in those of patients with osteoarthritis, who lack hyperplasia and inflammatory cell infiltration. In our study, we found expression of SDF-1 mRNA in joint tissue extracts of mice with signs of arthritis. This clearly suggests a role for SDF-1 in the invasion of leukocytes into the inflamed joint tissues (5, 6, 21). These findings are in line with our observation that, in mice sensitized to develop CIA, injection of SDF-1 in the footpad resulted in an inflammatory swelling reaction that was inhibited by AMD3100.

SDF-1 was originally cloned from a bone marrow stromal cell line (22) and found to act as a B cell growth factor (23). It was later found also to induce chemotaxis of immunocompetent (3) and progenitor cells (24) and to be involved in myelopoiesis (25, 26). However, we found no evidence to support the concept that in the CIA model, AMD3100 interfered with myelopoiesis and B cell growth. First, flow cytometric analysis evaluating the following markers (CD11b, CD19, B220, CD4, and CD8) did not reveal effects of AMD3100 on the proportions of Mac-1<sup>+</sup>, B, or T cell populations in spleen, blood, and bone marrow. In addition, cytospin preparations of spleen and bone marrow cell suspensions failed to reveal any effect of the drug on the numbers of immature myeloid cells (data not shown).

We also assessed whether SDF-1 and AMD3100 could interfere with osteoclastogenesis, which was recently reported to represent an important event in the pathogenesis of adjuvant-induced joint destruction (27). AMD3100 (20  $\mu\text{g}/\text{ml}$ ) failed to affect osteoclast formation induced in bone marrow and spleen cultures by stimulation with either osteoclast differentiation factor or TNF- $\alpha$ . In this setting, SDF-1 was unable to induce the formation of tartrate-resistant acid phosphatase-positive osteoclast-like cells (data not shown); therefore, it seems unlikely that SDF-1 or CXCR4 is involved in osteoclastogenesis.

Our observations provide evidence for a proinflammatory role of SDF-1 in vivo, and suggest that AMD3100 or similar specific inhibitors of SDF-1/CXCR4 may be useful not only for the treatment of rheumatoid arthritis, but also for the treatment of certain DTH-mediated allergies. However, before tests in patients can be

considered, evidence for activity in animals with an intact IFN- $\gamma$  system is needed, and strict absence of toxic side effects should be demonstrated.

## Acknowledgments

We thank C. De Wolf-Peeters for histological examinations; J. Van Damme for critical review of the manuscript; and T. Mitera, E. Fonteyn, B. De Klerck, and H. Vankelecom for excellent assistance or helpful discussions. We are indebted to S. Huang for providing the IFN- $\gamma$ R KO mice.

## References

- Zlotnik, A., and O. Yoshie. 2000. Chemokines: a new classification system and their role in immunity. *Immunity* 12:121.
- Bleul, C. C., M. Farzan, H. Choe, C. Parolin, I. Clark-Lewis, J. Sodroski, and T. Springer. 1996. The lymphocyte chemoattractant SDF-1 is a ligand for LESTR/fusin and blocks HIV-1 entry. *Nature* 382:829.
- Oberlin, E., A. Amara, F. Bachelier, C. Bessia, J. L. Virelizier, F. Arenzana-Seisdedos, O. Schwartz, J.-M. Heard, I. Clark-Lewis, D. F. Legler, et al. 1996. The CXC chemokine SDF-1 is the ligand for LESTR/fusin and prevents infection by T-cell-line-adapted HIV-1. *Nature* 382:833.
- Rossi, D., and A. Zlotnik. 2000. The biology of chemokines and their receptors. *Annu. Rev. Immunol.* 18:217.
- Buckley, C. D., N. Amft, P. F. Bradfield, D. Pilling, E. Ross, F. Arenzana-Seisdedos, A. Amara, S. J. Cumow, J. M. Lord, D. Scheel-Toellner, and M. Salmon. 2000. Persistent induction of the chemokine receptor CXCR4 by TGF- $\beta$ 1 on synovial T cells contributes to their accumulation within the rheumatoid synovium. *J. Immunol.* 165:3423.
- Nanki, T., K. Hayashida, H. S. El-Gabalawy, S. Suson, K. Shi, H. J. Girschik, S. Yavuz, and P. E. Lipsky. 2000. Stromal cell-derived factor-1-CXC chemokine receptor 4 interactions play a central role in CD4<sup>+</sup> T cell accumulation in rheumatoid arthritis synovium. *J. Immunol.* 165:6590.
- De Clercq, E., N. Yamamoto, R. Pauwels, M. Baba, D. Schols, H. Nakashima, J. Balzarini, B. A. Murrer, D. Schwartz, D. Thornton, et al. 1992. Potent and selective inhibition of human immunodeficiency virus (HIV)-1 and HIV-2 replication by a class of bicyclams interacting with a viral uncoating event. *Proc. Natl. Acad. Sci. USA* 89:5286.
- De Clercq, E., N. Yamamoto, R. Pauwels, J. Balzarini, M. Witvrouw, K. De Vreese, Z. Debyser, B. Rosenwirth, P. Peichl, R. Datema, et al. 1994. Highly potent and selective inhibition of human immunodeficiency virus by the bicyclam derivative AM3100. *Antimicrob. Agents Chemother.* 38:668.
- Hendrix, C. W., C. Flexner, R. T. MacFarland, C. Giandomenico, E. J. Fuchs, E. Redpath, G. Bridger, and G. Henson. 2000. Pharmacokinetics and safety of AMD-3100, a novel antagonist of the CXCR-4 chemokine receptor, in human volunteers. *Antimicrob. Agents Chemother.* 44:1667.
- Schols, D., S. Struyf, J. Van Damme, J. Esté, G. Henson, and E. De Clercq. 1997. Inhibition of T-tropic HIV strains by selective antagonization of the chemokine receptor CXCR4. *J. Exp. Med.* 186:1383.
- Donzella, G. A., D. Schols, S. W. Lin, J. A. Este, K. A. Nagashima, P. J. Maddon, G. P. Allaway, T. P. Sakmar, G. Henson, E. De Clercq, and J. P. Moore. 1998. AMD3100, a small molecule inhibitor of HIV-1 entry via the CXCR4 co-receptor. *Nat. Med.* 4:72.
- Feng, Y., C. C. Broder, P. E. Kennedy, and E. A. Berger. 1996. HIV-1 entry cofactor: functional cDNA cloning of a seven-transmembrane, G protein-coupled receptor. *Science* 272:872.
- Datema, R., L. Rabin, M. Hincenberghs, M.-B. Moreno, S. Warren, V. Linquist, B. Rosenwirth, J. Seifert, and J. M. McCune. 1996. Antiviral efficacy in vivo of the anti-human immunodeficiency virus bicyclam SDZ SID 791 (JM 3100), an inhibitor of infectious cell entry. *Antimicrob. Agents Chemother.* 40:750.
- Vermeire, K., H. Heremans, M. Vandeputte, J. Huang, A. Billiau, and P. Matthys. 1997. Accelerated collagen-induced arthritis in interferon- $\gamma$  receptor-deficient mice. *J. Immunol.* 158:5507.
- Manoury-Schwartz, B., G. Chiochia, N. Bessis, O. Abehsira-Amar, F. Batteux, S. Muller, S. Huang, M.-C. Boissier, and C. Fournier. 1997. High susceptibility to collagen-induced arthritis in mice lacking IFN- $\gamma$  receptors. *J. Immunol.* 158:5501.
- Matthys, P., K. Vermeire, T. Mitera, H. Heremans, J. Huang, D. Schols, C. Dewolf-Peeters, and A. Billiau. 1999. Enhanced autoimmune arthritis in IFN- $\gamma$  receptor-deficient mice is conditioned by mycobacteria in Freund's adjuvant and by increased expansion of Mac-1<sup>+</sup> myeloid cells. *J. Immunol.* 163:3503.
- Huang, S., W. Hendriks, A. Althage, S. Hemmi, H. Bluethmann, R. Kamijo, J. Vilcek, R. M. Zinkernagel, and M. Aguet. 1993. Immune response in mice that lack the interferon- $\gamma$  receptor. *Science* 259:1742.
- Vermeire, K., L. Thielemans, P. Matthys, and A. Billiau. 2000. The effects of NO synthase inhibitors on murine collagen-induced arthritis do not support a role of NO in the protective effect of IFN- $\gamma$ . *J. Leukocyte Biol.* 68:119.
- Taylor, P. C., C.-Q. Chu, C. Plater-Zyberk, and R. N. Maini. 1996. Transfer of type II collagen-induced arthritis from DBA/1 to severe combined immunodeficiency mice can be prevented by blockade of Mac-1. *Immunology* 88:315.
- Biermann, H., B. Pietz, R. Dreier, K. W. Schmid, C. Sorg, and C. Sunderkotter. 1999. Murine leukocytes with ring-shaped nuclei include granulocytes, monocytes, and their precursors. *J. Leukocyte Biol.* 65:217.
- Seki, T., J. Selby, and R. Winchester. 1998. Use of differential subtraction method to identify genes that characterize the phenotype of cultured rheumatoid arthritis synovioocytes. *Arthritis Rheum.* 41:1356.
- Tashiro, K., H. Tada, R. Heilker, M. Shirozu, T. Nakano, and T. Honjo. 1993. Signal sequence trap: a cloning strategy for secreted proteins and type I membrane proteins. *Science* 261:600.
- Nagasawa, T., H. Kikutani, and T. Kishimoto. 1994. Molecular cloning and structure of the pre-B-cell growth-stimulating factor. *Proc. Natl. Acad. Sci. USA* 91:2305.
- Aiuti, A., I. J. Webb, C. Bleul, T. Springer, and M. C. Gutierrez-Ramos. 1997. The chemokine SDF-1 is a chemoattractant for human CD34<sup>+</sup> hematopoietic progenitor cells and provides a new mechanism to explain the mobilization of CD34<sup>+</sup> progenitors to peripheral blood. *J. Exp. Med.* 185:111.
- Nagasawa, T., S. Hirota, K. Tachibana, N. Takakura, S. Nishikawa, Y. Kitamura, N. Yoshida, H. Kikutani, and T. Kishimoto. 1996. Defects of B-cell lymphopoiesis and bone-marrow myelopoiesis in mice lacking the CXC chemokine PBSF/SDF-1. *Nature* 382:635.
- Ma, Q., D. Jones, P. R. Borghesani, R. A. Segal, T. Nagasawa, T. Kishimoto, R. T. Bronson, and T. A. Springer. 1998. Impaired B-lymphopoiesis, myelopoiesis, and derailed cerebellar neuron migration in CXCR4- and SDF-1-deficient mice. *Proc. Natl. Acad. Sci. USA* 95:9448.
- Kong, Y. Y., U. Feige, I. Sarosi, B. Bolon, A. Tafuri, S. Morony, C. Caparelli, R. Elliott, S. McCabe, T. Wong, et al. 1999. Activated T cells regulate bone loss and joint destruction in adjuvant arthritis through osteoprotegerin ligand. *Nature* 402:304.